EUROfusion

EUROFUSION CP(15)04/15

N. Lemahieu et al.

Thermal Shock Behaviour of H and H/He-Exposed Tungsten at High Temperature

(18th May 2015 – 22nd May 2015)
Aix-en-Provence, France

This work has been carried out within the framework of the EUROfusion Consortium and has received funding from the Euratom research and training programme 2014-2018 under grant agreement No 633053. The views and opinions expressed herein do not necessarily reflect those of the European Commission.

PFMC-15

Thermal shock behaviour of H and H/He-exposed tungsten at high temperature

N Lemahieu[1,2,3], H Greuner[4], J Linke[1], H Maier[4], G Pintsuk[1], M Wirtz[1], G Van Oost[2] and J-M Noterdaeme[2,4]

[1] Forschungszentrum Jülich GmbH, Institut für Energie- und Klimaforschung, 52425 Jülich, Germany

[2] Department of Applied Physics, Ghent University, St.-Pietersnieuwstraat 41 B4, 9000 Ghent, Belgium

[3] Institute of Interfacial Process Engineering and Plasma Technology IGVP, Universität Stuttgart, Pfaffenwaldring 31, 70569 Stuttgart, Germany

[4] Max-Planck-Institut für Plasmaphysik, Boltzmannstraße 2, 85748 Garching, Germany

E-mail: `n.lemahieu@fz-juelich.de`

Abstract. Polycrystalline tungsten samples were characterized and exposed to a pure H beam or mixed H/He beam of containing 6% He in GLADIS. After 5400 s of exposure time with a heat flux of 10.5 MW/m^2, the total accumulated fluence of 2×10^{25} m^{-2} was reached. Thereafter, ELM-like thermal shocks with a duration of 1 ms and an absorbed power density of 190 MW/m^2 and 380 MW/m^2 were applied on the samples in JUDITH 1. During the thermal shocks, the base temperature was kept at 1000°C. The experiments with the lowest power density did not result in any detected damage. The other tests showed the beginning of crack formation, or in the case of one sample just roughening. This damage behaviour is similar, although slightly more pronounced, to the behaviour of samples that are subjected to identical ELM-like thermal shocks without being pre-exposed to a particle flux.

PACS numbers: 28.52.Fa, 52.40.Hf, 52.55.Rk, 61.80.Fe, 61.80.Jh

1. Introduction

Currently, tungsten is considered as one of the few plasma-facing materials (PFMs) which is suitable for both current and next-generation fusion reactors. Tokamaks like JET and ASDEX Upgrade already use tungsten as PFM. The ITER-operation will start with a full tungsten divertor. Furthermore, also for future reactors, e.g. DEMO, tungsten will stay a promising PFM [1].

Despite the advantages of tungsten, e.g. low erosion rate, high melting point, and low tritium retention, there are also known drawbacks, e.g. plasma contamination and brittleness. During the operation of a fusion reactor, tungsten will be subjected to a combination of loading conditions, including neutron and particle irradiation, steady state heat fluxes, and transient heat fluxes. Each loading condition can damage tungsten, change the surface morphology, and modify the material properties [2, 3].

To investigate the influence of the different exposure conditions, tungsten was tested in several ways, e.g. by electron beam facilities or linear plasma devices. To study how each exposure condition affects the PFMs, various experiments focussed on one loading condition [4–6]. Although these experiments are necessary to understand the separate loads, the overall performance of tungsten as PFM strongly depends on the synergistic effects of the combined loads. For this reason, experiments were carried out in which tungsten was exposed simultaneously or successively to several exposure types [7–9].

An important interaction might occur between edge localized modes (ELMs), which could lead to surface roughening, cracking, etc. [10], and steady state power and particle loading, which may result in bubble formation, surface morphology modifications, etc. [11]. As a consequence, the thermal shock behaviour of tungsten that was exposed to H and He particles beforehand, both performed at operation relevant surface temperatures, needs to be understood and will be addressed hereafter.

2. Experimental set-up

The used material was cut from a 99.97 wt% pure tungsten disk with a height of ~ 45 mm and a radius of ~ 72 mm. This double-forged disk, characterized by a microstructure with elongated grains, was manufactured by Plansee. Three rectangular cuboid shapes, with a height of 5 mm for S-samples, 10 mm for M-samples, and 15 mm for L-samples, were chosen as sample geometry. Each surface of the samples was 5 mm by 10 mm. All samples were cut with a longitudinal grain-orientation. This means that the elongation of the grains is parallel to the surface. After polishing, the sample surfaces have a maximal arithmetic mean roughness (R_a) of 0.1 μm.

The exposure of the samples to a steady state particle and heat flux was done in the high heat flux facility GLADIS at the Max-Planck-Institut für Plasmaphysik [12]. A Gaussian beam was used that has a particle flux of $3.7 \times 10^{21}\,\mathrm{m^{-2}s^{-1}}$ at its centre. Through several 30 s long pulses, a total exposure time of 90 min was achieved, which corresponds to a fluence of $2 \times 10^{25}\,\mathrm{m^{-2}}$ at the beam maximum. The beam contained

either only H or a mixed H/He composition with 6% He. A 30 kV extraction voltage resulted for both cases in a heat flux of 10.5 MW/m^2 at the beam centre.

The ion distribution for the pure H beam is 35% H atoms of 10 keV, 43% H atoms of 15 keV and 22% H atoms of 30 keV, resulting in a mean particle energy of 17 keV. For the mixed H/He-loading, is the energy distribution of H atoms considered similar to that of the pure H beam. Since spectroscopy only showed a Doppler shift from He^+, the He atoms have an energy of 30 keV [11]. The energy of the impinging particles in GLADIS is therefore higher than the mean energy of the steady-state loading in a tokamak plasma, which is several 10 eV. While this could mean that the resulting damage is not the same, experiments have shown that the surface morphology changes due to incident He atoms can be similar for both energy ranges [13].

The samples were brazed upon an actively cooled CuCrZr structure. Therefore, the sample height determines the surface temperature during exposure. L-samples reached the highest temperatures, 1500°C. For M-samples, the surface temperature was 1000°C, while it was 600°C for S-samples. This results in six loading conditions for GLADIS, originating from two different particle beams on three sample-types.

ELM-like thermal loading was performed in the JUDITH 1 electron beam facility at Forschungszentrum Jülich [14, 15]. During each pulse, a focussed electron beam scans a squared area measuring 4 mm by 4 mm on the sample surface for 1 ms. The loading spot moves on the surface in a triangular mode of 47 kHz in the x-direction and 43 kHz in the y-direction. Each sample was exposed to 100 identical pulses, which have an absorbed power density of either 190 MW/m^2 (HFF-6) or 380 MW/m^2 (HFF-12). A heater increased the sample temperature to 1000°C before the experiment started and kept it constant during the experiments. While the temperature of the bulk material was kept constant, the surface temperature in the loaded area rises during a pulse. For JUDITH 1, this results in two loading conditions.

At first, reference tests were performed with polished tungsten-samples. They were exposed to either the six GLADIS conditions or the two JUDITH 1 conditions. After obtaining these eight references, consecutive tests were executed. During these, pristine specimens were first exposed to GLADIS and thereafter in JUDITH 1, resulting in twelve different combinations. Due to a technical failure, the L-samples exposed in JUDITH 1 to HFF-6 could not be analysed. Post-mortem analysis of the thermal shock damage and the particle induced surface modifications was done with scanning electron microscopy (SEM), focussed ion beam (FIB), profilometry, and metallographic cross-sections.

3. Results and discussion

The GLADIS references correspond to the reference tests for earlier reported investigations of ELM-like damage at H or H/He exposed tungsten [16]. In all cases the sample surface was altered and an erosion pattern can be seen on SEM-pictures. Cross-sections of the L-samples showed grain growth up to ~ 3.5 mm deep, which did not happen for the S- and M-samples. While the average minimal and maximal Feret

Table 1. Arithmetic mean roughness R_a (μm) before thermal shocks, indicated by Pre-ELM, and after 100 thermal shocks at 1000°C, indicated by HFF-6 (190 MW/m^2) or HFF-12 (380 MW/m^2). The data is calculated from 50 points/mm profilometry.

Sample	Pre-ELM	HFF-6	HFF-12
Reference JUDITH 1	0.08	0.12	0.56
S-sample with H-flux	0.39	0.38	0.48
S-sample with H/He-flux	0.43	0.49	0.57
M-sample with H-flux	0.34	0.39	0.58
M-sample with H/He-flux	0.31	0.33	0.38
L-sample with H-flux	0.33	/	0.75
L-sample with H/He-flux	0.42	/	0.46

diameter was 25 μm and 63 μm for the as-received material, it became for the L-samples 59 μm and 99 μm after GLADIS exposure. The M- and L-samples exposed to a H/He-flux also exhibit protruding surface structures. FIB-sections of the samples showed also cavities, as observed during other GLADIS-experiments [11].

Analyses of the reference JUDITH 1 samples indicate that there is no damage after HFF-6 for 1000°C base temperature. Such a lack of damage is in accordance with earlier results of HFF-6 on the same material at room temperature or 400°C [16]. For the reference HFF-12 at 1000°C, as shown in figure 1, the surface is heavily deformed and the R_a, shown in table 1, increases. The fine lines on the surface are either the beginning of crack formation or height differences on the surface. Both are present on the reference sample, but not enough data is available to determine a typical crack depth. For example, crack initiations of around $\sim$ 300 nm depth are detected, as well as a crack which extends at least 6 μm deep, both shown in figure 1. These observations are in contrast with the damage behaviour at lower temperatures. After the HFF-12 pulses at temperatures where tungsten is ductile, only roughening occurs [10].

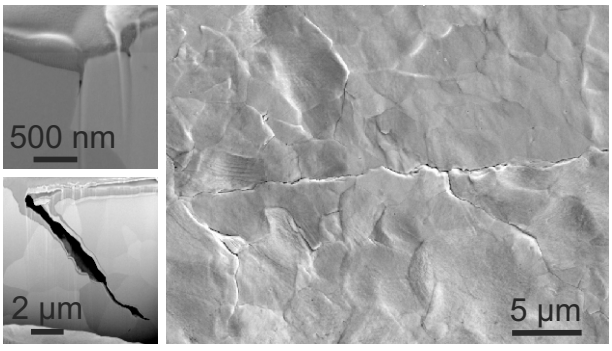

Figure 1. FIB-sections (left) and SEM (right) of pristine tungsten exposed to 100 pulses of HFF-12 at a base temperature of 1000°C.

Both SEM pictures and laser profilometry show no difference between GLADIS reference samples and the HFF-6 samples. Table 1 suggests an increased roughness for the S-sample with H/He-exposure and the M-sample with H-exposure. However,

the values differ by $\sim 0.05\,\mu$m from each other, which falls within the accuracy of the profilometry and is not considered an relevant increase. Metallographic cross-sections confirmed these conclusions. All post-mortem analyses show, similar to the JUDITH 1 reference, there is no damage after the low power density ELM-like loading.

All samples show surface modifications after the HFF-12 tests. This was either indicated by the R_a, see table 1, or by the SEM-pictures. Only the L-sample with H irradiation exhibited nothing more than surface roughening. This sample is then also the only one with a substantial higher R_a than the reference sample, although the increase in R_a is similar to the increase at the reference sample. The other samples show crack initiation similar to the JUDITH 1 reference sample, e.g. figure 2, although the width of these crack initiations varies and increases. For the M-sample with H/He-exposure, this is the most extreme with an average width of $0.53\,\mu$m and a standard deviation of $0.39\,\mu$m. The observation of roughening and/or crack initiations at HFF-12 demonstrates in combination with the lack of surface modifications at HFF-6, that the power density where any form of damage starts to occur, i.e. the damage threshold, does not change after H or H/He irradiation.

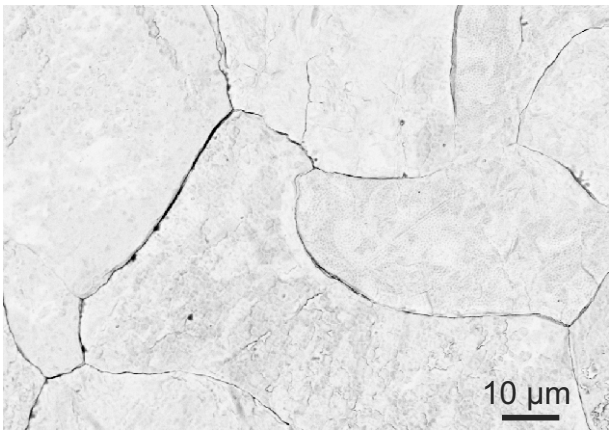

Figure 2. Tungsten surface of the M-sample with H exposure after 100 pulses of HFF-12 at a base temperature of 1000°C.

FIB-sections on the H/He-exposed samples, e.g. figure 3, show that the shallow cracks are in the $0.3 - 6\,\mu$m range observed with the JUDITH 1 reference. The deepest measured crack on the FIB-sections is $\sim 5\,\mu$m, while the smallest crack depth measurement is $0.42\,\mu$m. Furthermore, after this analysis it is observed that for the S-sample exposed to the H/He beam, the cavities present in the subsurface layer are altered and have grown.

The bubbles are compared with FIB-sections from the corresponding GLADIS reference sample and a GLADIS sample with JUDITH 1 exposure at room temperature and at the same power density, obtained in a previous experiment [16]. The FIB-analysis for these two samples show similar bubbles, only the cavities of the S-samples after the thermal shocks at 1000°C are different. This could be caused by heating up the base temperature to 1000°C for the duration of the experiments or it could be an effect of

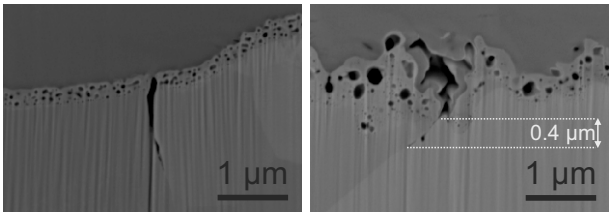

Figure 3. FIB-sections of the S-sample (left) and L-sample (right) with H/He-irradiation after HFF-12 pulses at a base temperature of 1000°C.

the thermal shocks at this temperature. While dedicated tests should be executed to pinpoint the cause, it is plausible to assume that the base temperature is a main factor. A potential explanation could be, if the cavity still contains gas, that even without a particle flux going to the material during the temperature rise, this could increase the gas pressure in the bubble. Furthermore, the shear modulus of tungsten decreases with increasing temperatures, reducing the required pressure for bubble growth according the Greenwood mechanical equilibrium condition [17, 18]. This might have resulted in bubble growth and explains why it only happened for the S-sample.

Also on the metallographic cross-sections no deep crack propagations are observed, as figure 4 shows for H-exposed samples. The beginning of cracks in the micrometer range is not detectable in these cross-sections, due to their limited depth and size. This is another indication that the thermal shock behaviour is not deteriorated for the particle exposed samples, in comparison with the JUDITH 1 reference sample.

Figure 4. From left to right, the cross-section of the S-, M-, and L-samples with H-exposure after HFF-12 pulses at a base temperature of 1000°C.

4. Conclusion

The ELM-like tests on pristine material at 1000°C showed, as it is the case for experiments at lower temperatures, no damage below 380 $\mathrm{MW/m^2}$ thermal shocks. The observed damage was not only surface roughening, but for most samples also the beginning of crack formation, unlike the cracks occurring at low base temperatures. The material pre-exposed to a particle flux had a similar thermal shock behaviour, although some of these shallow cracks indicate a faster development of damage. Even though

there is no damage deterioration, it is more pronounced and only experiments with higher pulse numbers could determine the extent of this increase.

In addition, this study found that the cavities of the H/He-exposed S-sample did grow after the JUDITH 1 exposure. Dedicated experiments will be necessary to resolve the responsible mechanism.

Acknowledgments

This work was supported by the European Commission and carried out within the framework of the Erasmus Mundus International Doctoral College in Fusion Science and Engineering (FUSION-DC). This work was executed under EUROfusion WP PFC. This work has been carried out within the framework of the EUROfusion Consortium and has received funding from the Euratom research and training programme 2014-2018 under grant agreement No 633053. The views and opinions expressed herein do not necessarily reflect those of the European Commission.

References

[1] Kaufmann M and Neu R 2007 *Fusion Engineering and Design* **82** 521–527
[2] Federici G, Skinner C H, Brooks J N, Coad J P, Grisolia C, Haasz A A, Hassanein A, Philipps V, Pitcher C S, Roth J, Wampler W R and Whyte D G 2001 *Nuclear Fusion* **41** 1967
[3] Philipps V 2011 *Journal of Nuclear Materials* **415** S2–S9
[4] Yoshida N, Iwakiri H, Tokunaga K and Baba T 2005 *Journal of Nuclear Materials* **337** 946–950
[5] Lemahieu N, Linke J, Pintsuk G, Van Oost G, Wirtz M and Zhou Z 2014 *Physica Scripta* **2014** 014035
[6] Yuan Y, Greuner H, Böswirth B, Krieger K, Luo G N, Xu H, Fu B, Li M and Liu W 2013 *Journal of Nuclear Materials* **433** 523–530
[7] Huber A, Wirtz M, Sergienko G, Steudel I, Arakcheev A, Burdakov A, Esser H G, Freisinger M, Kreter A, Linke J *et al.* 2015 *Fusion Engineering and Design* **in press**
[8] Loewenhoff T, Linke J, Pintsuk G, Pitts R and Riccardi B 2014 *Journal of Nuclear Materials* **in press**
[9] van Eden G, Morgan T, van der Meiden H, Matejicek J, Chraska T, Wirtz M and Temmerman G D 2014 *Nuclear Fusion* **54** 123010
[10] Linke J, Loewenhoff T, Massaut V, Pintsuk G, Ritz G, Rödig M, Schmidt A, Thomser C, Uytdenhouwen I, Vasechko V and Wirtz M 2011 *Nuclear Fusion* **51** 6p
[11] Greuner H, Maier H, Balden M, Linsmeier C, Böswirth B, Lindig S, Norajitra P, Antusch S and Rieth M 2013 *Journal of Nuclear Materials* **442** S256–S260
[12] Greuner H, Boeswirth B, Boscary J and McNeely P 2007 *Journal of Nuclear Materials* **367** 1444–1448
[13] Wright G, Brunner D, Baldwin M, Doerner R, Labombard B, Lipschultz B, Terry J and Whyte D 2012 *Nuclear Fusion* **52** 042003
[14] Duwe R, Kühnlein W and Münstermann H 1994 *Fusion Technology* 355–358
[15] Linke J, Bolt H, Duwe R, Kühnlein W, Lodato A, Rödig M, Schöpflin K and Wiechers B 2000 *Journal of Nuclear Materials* **283–287** 1152–1156
[16] Lemahieu N, Greuner H, Linke J, Maier H, Pintsuk G, Van Oost G and Wirtz M 2015 *Fusion Engineering and Design* **submitted**
[17] Greenwood G, Foreman A and Rimmer D 1959 *Journal of Nuclear Materials* **1** 305–324
[18] Sang C, Sun J, Bonnin X, Liu S and Wang D 2013 *Journal of Nuclear Materials* **443** 403–408